Electronic Supplementary Material (ESI) for Physical Chemistry Chemical Physics.

Supplementary Information

Surface-independent CO_2 and CO Reduction on Two-dimensional Kagome Metal KV_3Sb_5

Xin-Wei Chen, Zheng-Zhe Lin*, Meng-Rong Li

School of Physics, Xidian University, Xi'an 710071, China

* Corresponding Author. E-mail address: zzlin@xidian.edu.cn

1. The effect of various +*U* values on the energy bands

In this section, the calculation results of the energy bands via PBE functional is compared with the results via PBE +*U*. **Fig. S1** shows the energy bands of KV_3Sb_5 at the level of PBE and PBE +U (for U = 0, 0.5, 1, 1.56 and 3 eV). We find that with increasing U, the energy bands are deviating from their origin structures and these Dirac points become unnoticeable. Such similar situation also exist in the energy calculation of KV_3Sb_5 by Zhao et al [1]. They reported a dynamical mean-field theory (DMFT) study to produce energy bands without distortion. This phenomenon is common in metallic compounds with aggregated 3*d* elements.

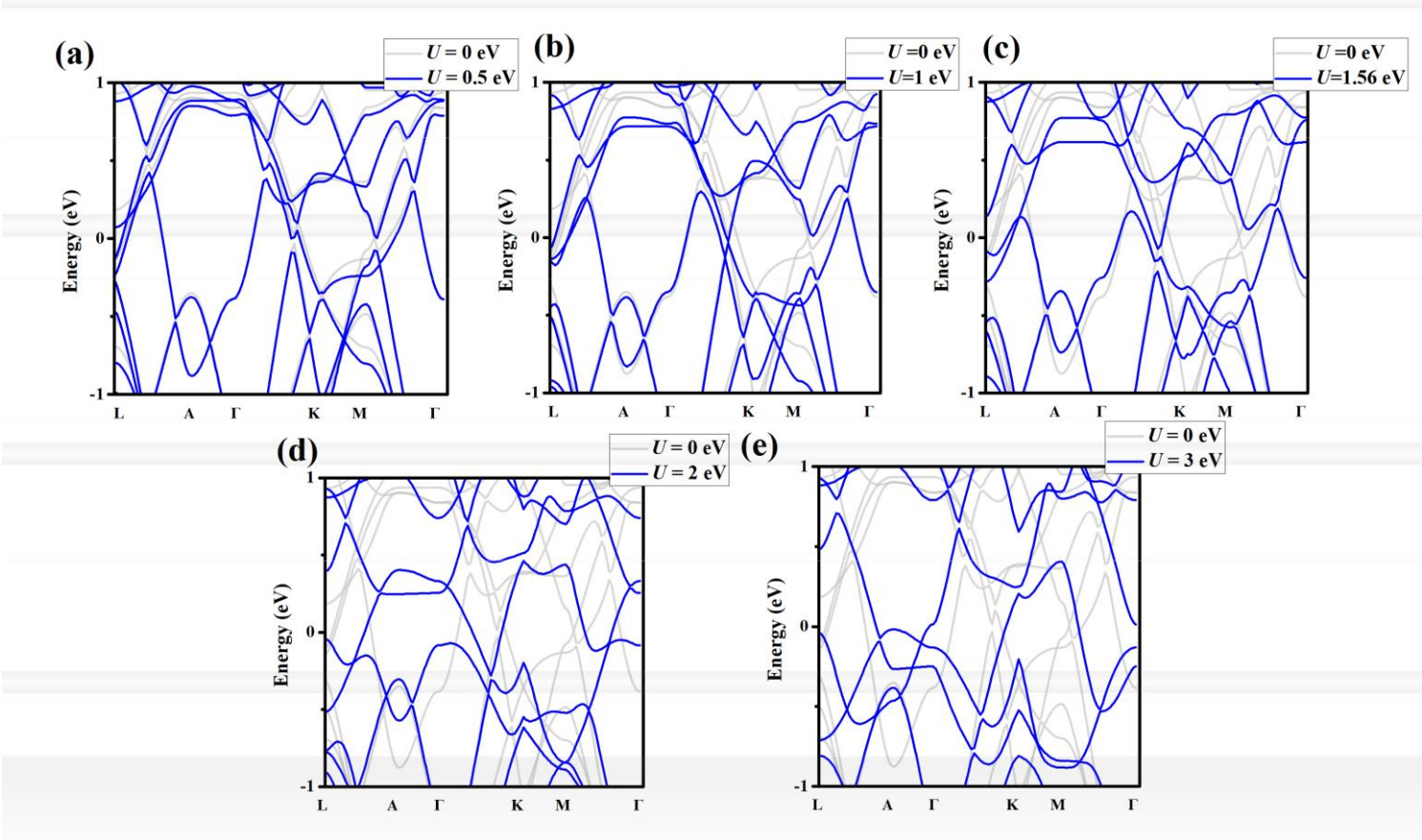

Fig. S1 The energy bands of KV_3Sb_5 at the level of PBE and PBE +*U*. The grey lines represent the energy bands calculated in PBE and the blue lines represent the energy bands calculated in PBE with various +*U*.

References:

[1] J. Zhao, W. Wu, Y. Wang, S. A. Yang, *Phys. Rev. B* **103**, L241117 (2021).

2. Determining the surface formation energy of KV_3Sb_5

In order to evaluate the stability of different surfaces, the chemical potential of the three atomic layers should be investigated. Their chemical potential are used to describe their interaction energy. To simplify the calculation, here we just consider the interaction between adjacent and second-adjacent layers. Hence, the equation of the free energy of KV_3Sb_5 in a unit cell is defined as

$$E(\text{cell}) = \mu_{K_0} + 2\mu_{Sb20} + \mu_{VSb10} + 4I_{K-Sb2} + 4I_{Sb2-VSb1} + 4I_{K-VSb1} + 4I_{Sb2-Sb2} \quad \text{(S1)}$$

where μ_{K_0}, μ_{Sb2_0} and μ_{VSb1_0} represent the chemical potential of K, Sb2 and VSb1 layers without interaction, respectively. The term $2I_{K-Sb2}$ represents the interaction energy between one K layer and one adjacent Sb2 layer, and so on. We supposed that the interaction energy is divided equally on the chemical potential of each layer. Hence, a K layer can interact with two adjacent Sb2 layer and be allocated chemical potential of $2I_{K-Sb2}$. The total chemical potential of K layer in bulk KV_3Sb_5 reads

$$\mu_K = \mu_{K_0} + 2I_{K-Sb2} + 2I_{K-VSb1} \quad \text{(S2)}$$

Similarly, the chemical potential of Sb2 and VSb1 layers are

$$\mu_{Sb2} = \mu_{Sb20} + I_{K-Sb2} + I_{Sb2-VSb1} + 2I_{Sb2-Sb2} \quad \text{(S3)}$$

and

$$\mu_{VSb1} = \mu_{VSb10} + 2I_{Sb2-VSb1} + 2I_{K-VSb1} \quad \text{(S4)}$$

The free energy of KV_3Sb_5 unit cell without one K layer reads

$$E(\text{without K}) = 2\mu_{Sb20} + \mu_{VSb10} + 4I_{Sb2-VSb1} + 4I_{Sb2-Sb2} \quad \text{(S5)}$$

Based on an optimized unit cell, we get rid of one or two layers in it and then perform static calculation. The formulas are listed in the following. The free energy of KV_3Sb_5 unit cell without one Sb2 layer reads

$$E(\text{without Sb2}) = \mu_{K_0 20} + \mu_{VSb10} + 2I_{K-Sb} + 2I_{Sb2-VSb1} + 4I_{K-VSb1} + \mu_{Sb} \quad \text{(S6)}$$

The free energy of KV_3Sb_5 unit cell without one VSb1 layer reads

$$E(\text{without VSb1}) = \mu_{K_0} + 2\mu_{Sb\,20} + 4I_{K-Sb\,2} + 4I_{Sb2-Sb2} \quad \text{(S7)}$$

The free energy of KV_3Sb_5 unit cell without one VSb1 and one K layer reads

$$E(\text{without K and VSb1 }) = \quad 2\mu_{Sb20} + 4I_{Sb2-Sb2} \tag{S8}$$

The free energy of KV_3Sb_5 unit cell without one Sb2 and one K layer reads

$$E(\text{without K and Sb2}) = \quad \mu_{Sb20} + \mu_{VSb10} + 2I_{Sb2-VSb1} \tag{S9}$$

The free energy of KV_3Sb_5 unit cell without one Sb2 and one VSb1 layer reads

$$E(\text{without VSb1 and Sb2}) = \quad \mu_{K_0} + \mu_{Sb20} + 2I_{K-Sb2} \tag{S10}$$

The linear relation above can be summarized into the following matrix formula,

$$\begin{pmatrix} E(\text{cell}) \\ E(\text{without K}) \\ E(\text{without Sb2}) \\ E(\text{without VSb1}) \\ E(\text{without K and VSb1}) \\ E(\text{without K and Sb2}) \\ E(\text{without Sb2 and VSb1}) \end{pmatrix} = \begin{pmatrix} 1 & 2 & 1 & 4 & 4 & 4 & 4 \\ 0 & 2 & 1 & 0 & 4 & 0 & 4 \\ 1 & 1 & 1 & 2 & 2 & 4 & 0 \\ 1 & 2 & 0 & 4 & 0 & 0 & 4 \\ 0 & 2 & 0 & 0 & 0 & 0 & 4 \\ 0 & 1 & 1 & 0 & 2 & 0 & 0 \\ 1 & 1 & 0 & 2 & 0 & 0 & 0 \end{pmatrix} \begin{pmatrix} \mu_{K^0} \\ \mu_{Sb2_0} \\ \mu_{VSb1_0} \\ I_{K-Sb2} \\ I_{Sb2-VSb1} \\ I_{K-VSb1} \\ I_{Sb2-Sb2} \end{pmatrix}$$

According to the results of static calculation, seven energy values on the left are E(cell) = −45.651 eV, E(without K) = −43.143 eV, E(without Sb2) = −34.584 eV , E(without VSb1) = −16.424eV, E(without K and VSb1) = −13.2517 eV, E(without K and Sb2) = −32.293 eV and E(without Sb2 and VSb1) = −9.024eV. Calculated by inversing the matrix, μ_{K_0}, μ_{Sb2_0}, μ_{VSb1_0}, I_{K-Sb2}, $I_{Sb2-VSb1}$, I_{K-VSb1} and $I_{Sb2-Sb2}$ are −2.74 eV, −6.07 eV, −22.56 eV, −0.11 eV, −1.83 eV, 0.16 eV and −0.28eV, respectively. Using **Eq. (S2)**, **(S3)** and **(S4)**, the chemical potentials μ_K, μ_{Sb2_0} and μ_{VSb1_0} are −2.62 eV, −8.57 eV and −25.89 eV, respectively.

3. Active sites on the surfaces

To understand the surface activity of KV_3Sb_5, here we analyze the formation energies of H* and O* absorbed on different sites A, B, C and D for the three surfaces (for the definition of surfaces and sites, see **Fig. 3(a)**), namely perfect surface Sb2-VSb1, surface Sb2-VSb1 with Sb vacancy, and perfect surface VSb1. Here, A is on the top of an Sb atom in the VSb1 layer. B is on the top of an Sb atom in Sb2 layer. the V triangle in the VSb1 layer. D is on the top of a V atom in the VSb1 layer. For surface Sb2-VSb1, A and B sites are considered. When with Sb vacancy, the exposed C site in the second layer is then considered too. For surface VSb1, A, C and D sites are considered. The equation of formation energy can be written as

$$\Delta G(\mathrm{H}^*) = G(\mathrm{H}^*) - G(\mathrm{slab}) - \frac{1}{2}G(\mathrm{H_2}) + eU$$

and $$\Delta G(\mathrm{O}^*) = G(\mathrm{O}^*) - G(\mathrm{slab}) + G(\mathrm{H_2}) - G(\mathrm{H_2O}) - 2eU$$

According to their formation energy (listed in **Table S1**), we can find that both for H* and O* on the perfect Sb2-VSb1 surface, their formation energies for A site are lower that for B site. But with a vacancy of Sb atom on the surface, the C site is exposed and O* as well as H* is more easily absorbed here. For the completely exposed VSb1 surface, the hollow site C is better than other sites.

Table S1 The Formation energy of H* and O* absorbed on different sites.

Surfaces	Sb2-VSb1		Sb2-VSb1 with vacancy			VSb1		
Sites	A	B	A	B	C	A	C	D
ΔG(H*) (eV)	0.55	1.42	0.67	1.25	-0.62	2.58	-0.78	0.60
ΔG(O*) (eV)	1.34	1.76	1.24	1.80	-1.53	2.01	-1.81	-0.26

In conclusion, the most active sites on these surfaces are A for perfect surface Sb2-VSb1, C for surface VSb1 and surface Sb2-VSb1 with Sb vacancy.

4. The main products of CO_2RR and CORR

In this section, we introduce the main product and reaction in CO2RR and CORR. Considering the market mass and economic viability, CO and HCOOH are the main product through COOH path and HCOO path respectively. The product CO can act as a substrate to undergo the process of CO reduction reaction. For the multicarbon products, they are difficult to obtain in CO_2RR but CORR provide a better route for the formation of multicarbon product [1]. **Table S2** shows the product and reaction of CO_2RR. Except for CO and HCOOH, CO_2RR share the same products with CORR.

Table S2 The reactions and products of CO_2RR.

Product	Reaction
HCOOH	$CO_2 + H_2 \rightarrow HCOOH$
CO	$CO_2 + H_2 \rightarrow CO + H_2O$
CH_4	$CO_2 + 4H_2 \rightarrow CH_4 + 2H_2O$
HCHO	$CO_2 + 2H_2 \rightarrow HCHO + H_2O$
C_2H_4	$2CO_2 + 6H_2 \rightarrow C_2H_4 + 4H_2O$
CH_3CH_2OH	$2CO_2 + 6H_2 \rightarrow CH_3CH_2OH + 3H_2O$
C_2H_6	$2CO_2 + 7H_2 \rightarrow C_2H_6 + 4H_2O$
C_3H_7OH	$3CO_2 + 9H_2 \rightarrow C_3H_7OH + 5H_2O$
CH_3OH	$CO_2 + 3H_2 \rightarrow CH_3OH + H_2O$

References:

[1] Y. Meng, S. B. Cheng, Z. Wu, *Appl. Surf. Sci.* **597**, 153761 (2022).

5. CO_2RR and CORR on pristine surfaces K and VSb1

Although the surface K cannot exist in aqueous electrolyte, we still roughly investigate the catalytic performance without considering its surface states. Simultaneously, the pristine surface VSb1 is also discussed as a control. Their intermediates and free energies are shown in **Fig. S2 (a) - (d)**. From the data, we can easily find that compared with the surface K, the surface VSb1 has a stronger adsorption capacity for the intermediates in CO_2RR and CORR because the free energy for the intermediates absorbed on the surface gradually decreases as the reduction reaction proceeds. Their free energies are lower than those of the same intermediates on the K surface. For the intermediate HCOO* on K surface, the two O atoms are on the bridge sites of K atoms. On the VSb1 surface, only one atom is on the hollow site of the V triangle. Such the bridge connection brings the absorbed HCOO* lower energy. As a rate-determining reaction step $HCOO^* + H^+ + e^- \rightarrow HCOOH^*$, the free energy rises sharply by 1.77 eV. Such a large onset potential used in CO_2RR is just a waste of electric energy. We also find the two O atoms in HCOOH* move closer to K atom. The change of their position might contribute to the rise in free energy. For the H_2COOH^*, the O atoms return to the bridge site and its free energy decreases. The next step, the C-OH bond in HCOOH is cut by H and H_2CO^* forms, which also appears in the CORR.

For the CORR on the K surface, the rate-determining step is $HCO^* + H^+ + e^- \rightarrow H_2CO^*$ with an increase in free energy by 0.31 eV. The following steps are energy-decreasing. The desorption of H_2CO^* requires 0.38 eV. Hence, it is more likely to be reduced to H_3CO^* and finally to $CH_4 + H_2O(aq)$. The O* cannot exist when $U < 0$ V. But for CORR on VSb1 surface, the final product is also CH_4 but the O* remains because of its strong connection with the V atoms in the site. This is the reason why we had to consider the states of VSb1 surface.

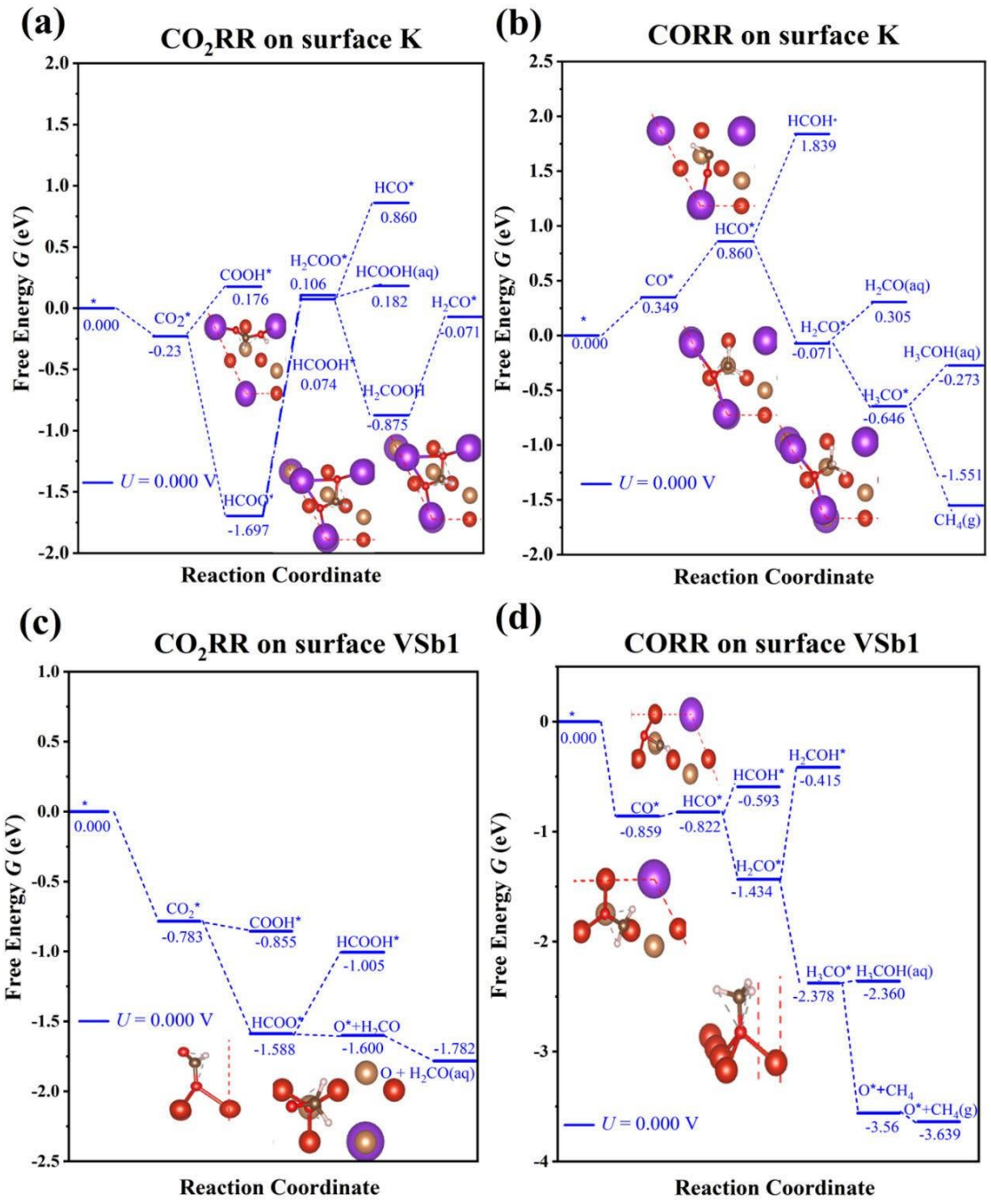

Fig. S2 The free energies of reaction intermediates on the pristine K surface for CO_2RR and CORR as well as on the pristine VSb1 surface for CO_2RR and CORR.

6. The surface formation energy

To verify the results of KV_3Sb_5 surface formation energy, we compare the data with the surface formation energies of common metals. The experimentally measured surface energies of transition metals are in the range of 1~3 J/m^2, while the surface energies of most main-group metals are below 1 J/m^2 [1]. The formation energies of KV_3Sb_5 surfaces are within this range.

As a comparison, we calculate the surface formation energy of Cu (111) surface. The Cu lattice is face-centered cubic. The primitive cell of Cu is shown in **Fig. S3 (a)**. The six-layer slab model shown in **Fig. S3 (b)** has exposed Cu (111) surfaces at both ends. The calculation is performed at the level of PBE, with a kinetic energy cut-off of 500 eV. The Brillouin zone is sampled with a k-spacing of 0.04 Å^{-1}. The geometries of bulk and slab models are relaxed. The surface formation energy of the Cu (111) surface is determined to be 7.58×10^{-2} eV/Å^2, which is equivalent to 1.22 J/m^2 in SI unit. This result is close to the calculation in Ref. 2.

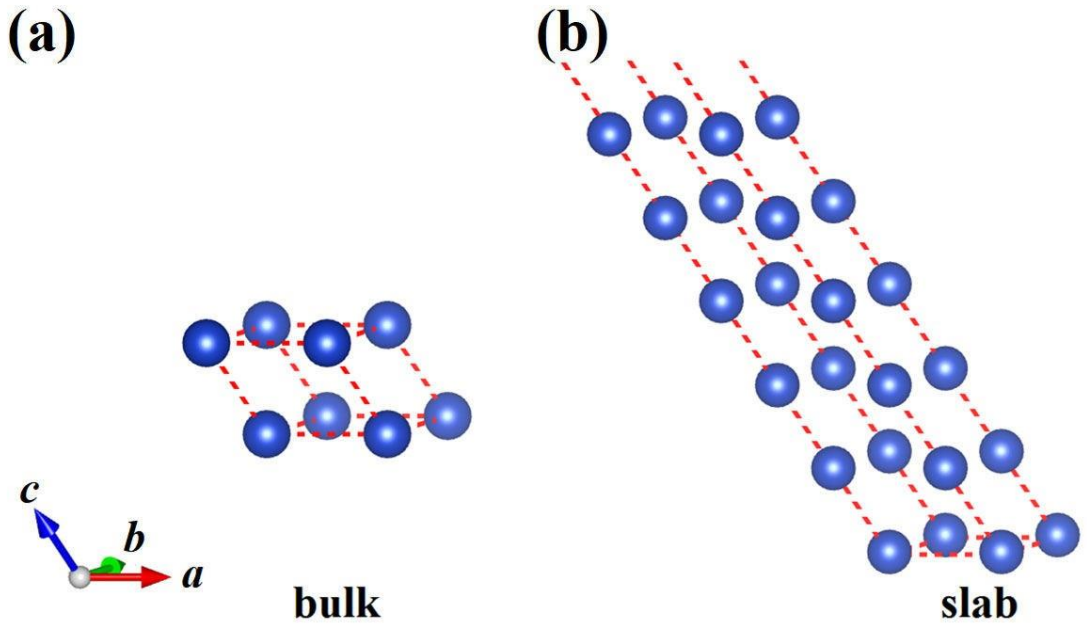

Fig. S3 The models of bulk Cu and a slab of the Cu (111) surface.

It should be noted that the surface formation energy is positive, which means that creating a surface from bulk materials is endothermic. The (111) surface is a commonly

exposed surface of Cu grains. For KV_3Sb_5, the calculated formation energies of the K and Sb2-VSb1 surfaces are lower than that of the Cu (111) surface. This indicates that the K and Sb2-VSb1 surfaces should be more stable. The Sb2-K and VSb1 surfaces are less stable, as indicated by their higher formation energies.

References:

[1] L. Vitos, A. V. Ruban, H. L. Skriver, J. Kollár, *Surf. Sci.* **411**, 186-202 (1998).

[2] Y. Han, K. C. Lai, A. Lii-Rosales, M. C. Tringides, J. W. Evans, P. A. Thiel, *Surf. Sci.* **685**, 48-58 (2019).

7. Solvation effect and the explicit solvent model

Chemical reactions at the interface between solid and liquid are always affected by the solvation effect. In theoretical simulations, the solvation effect can be simplified using the implicit solvent model, which primarily considers the effect of solvent molecules as dielectric. Although this method reduces the quantity of computation, its reliability should be verified. Indeed, the solvation effect is essential for the reactions. In an aqueous environment, hydrogen bonding between water molecules and the reaction intermediate has a significant effect in certain cases. This effect is not accounted for in the implicit solvent model. The explicit model should include at least one or two solvent layers, preferably containing more than three layers. Moreover, for a certain reaction intermediate, many different configurations of solvent molecules should be considered in order to find the lowest-energy configuration. This results in a large computation quantity.

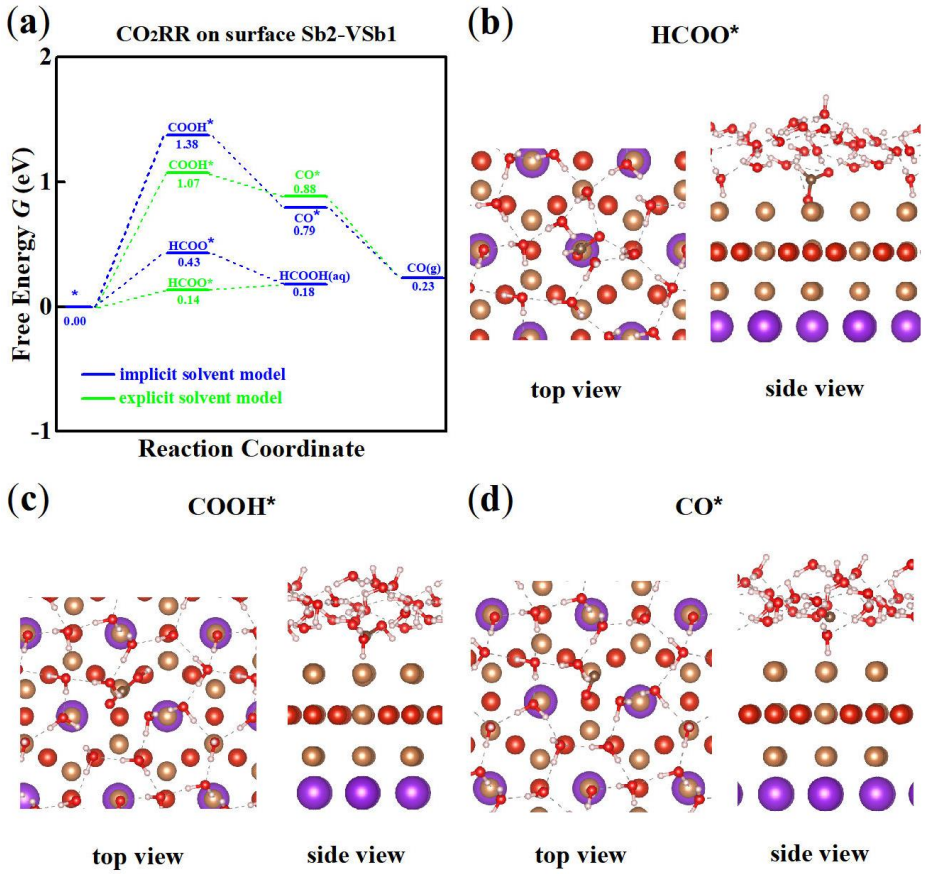

Fig. S4 (a) The reaction free energy of CO_2RR on surface Sb2-VSb1, calculated using the explicit and implicit solvent model. The structure of **(b)** HCOO*, **(c)** COOH* and **(d)** CO* in the explicit solvent model.

The slab models in our study contain more than one hundred atoms. It is difficult to calculate every reaction intermediate using the explicit model. In this section, some typical reaction processes are dealt with the explicit water model, and compared with the results of implicit model. The calculation using the explicit water model employs two layers of water molecules. **Fig. S4 (a)** shows the free energy diagram of CO_2RR on the Sb2-VSb1 surface. The data from the explicit and implicit models are both shown for comparison. The free energies of COOH* and HCOO* given by the explicit model are correspondingly lower than those given by the implicit model. In **Fig. S4 (b)** and **(c)**, we can see the hydrogen bonds between water molecule and the COOH* and HCOO*. This is the reason for the stabilization of COOH* and HCOO*. In contrast, the free energy of CO* calculated by the explicit model is higher than that by the implicit model due to the hydrophobicity of CO*.

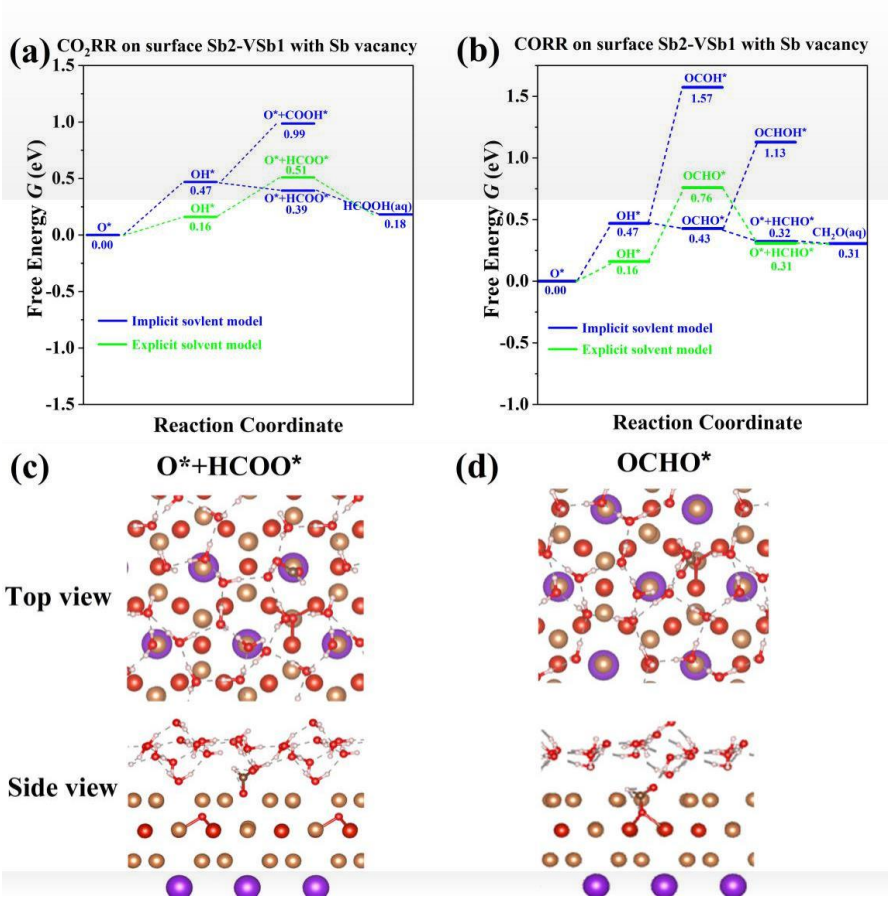

Fig. S5 The reaction free energy of **(a)** CO_2RR and **(b)** CORR on surface Sb2-VSb1 with Sb vacancy, calculated using the explicit and implicit solvent model. The structure of **(c)** O*+HCOO* and **(d)** OCHO* in the explicit solvent model.

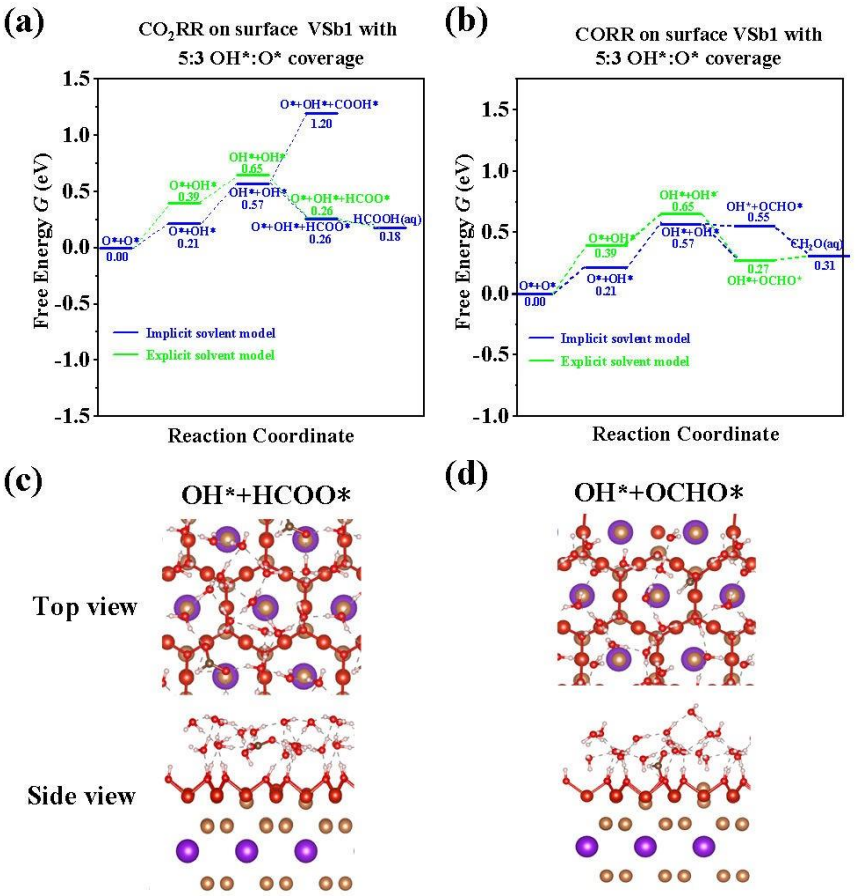

Fig. S6 The reaction free energy of **(a)** CO_2RR and **(b)** CORR on the surface VSb1 with a 5:3 OH*:O* coverage, calculated using the explicit and implicit solvent model. The structure of **(c)** OH*+HCOO* and **(d)** OH*+OCHO* in the explicit solvent model.

For CO_2RR and CORR on the Sb2-VSb1 surface with an Sb vacancy, we can observe the effect of hydrogen bonding on O*. **Fig. S5 (a)** and **(b)** show the free energy diagrams of CO_2RR and CORR, respectively, on the Sb2-VSb1 surface with an Sb vacancy. For the initial state O* in the explicit water model, we observe a stabilization effect by the hydrogen bonding between O* and H_2O. For OH*, the free energy is lower compared to the implicit model due to the hydrogen bonding between the H of OH* and the O of H_2O molecule. In CO_2RR, the free energy of O*+HCOO* in the explicit model is larger than that in the implicit model. In **Fig. S5 (c)**, we can see a hydrogen bond between the O of HCOO* and the H of H_2O molecule. But the stabilization effect of hydrogen bonding for HCOO* is weaker than that of O*. So, the free energy of O*+HCOO* in the explicit water model is higher than that in the implicit model. For CORR, similar effect is also found for OCHO*. In **Fig. S5 (d)**, we can see a hydrogen

bond between OCHO* and H_2O. In **Fig. S5 (b)**, the free energy of OCHO* in the explicit model is larger than that in the implicit model.

Fig. S6 (a) and **(b)** show the free energy diagrams of CO_2RR and CORR, respectively, on the VSb1 surface with a 5:3 OH*:O* coverage. The explicit model shows larger free energy change for the O*→OH* steps. **Fig. S6 (c)** shows the structure of HCOO* in CO_2RR calculated by the explicit model. The free energy of HCOO* calculated by the explicit model is close to that of the implicit model. **Fig. S6 (d)** shows the structure of OCHO* in CORR calculated by the explicit model. The free energy of HCOO* calculated by the explicit model is much lower than that of the implicit model. We can also see the effect of hydrogen bonds.

In summary, in the presence of hydrogen bonding, we cannot expect the explicit and implicit models to be exactly the same. Qualitatively, the trends of free energy given by the explicit and implicit models are consistent. The HCOO* reaction path is actually thermodynamically favorable. To save computation quantity, we use the implicit model in the whole study.

8. **The H-shuttle mechanism**

In the step of O* + H^+ + e → OH*, we observe an indirect process of H transfer, known as the H-shuttle mechanism. For the initial state, if the H_3O^+ is placed near O*, it will transform into OH* in the geometry relaxation. In the stable configuration, the H_3O^+ should be located farther. The H_3O^+ is located at a position that is a distance away from the O* (separated by one or two H_2O). In the reaction path of O* + H^+ + e → OH*, the H is transferred from one H_2O to another, and then to the destination. **Fig. S7** and **S8** show two examples.

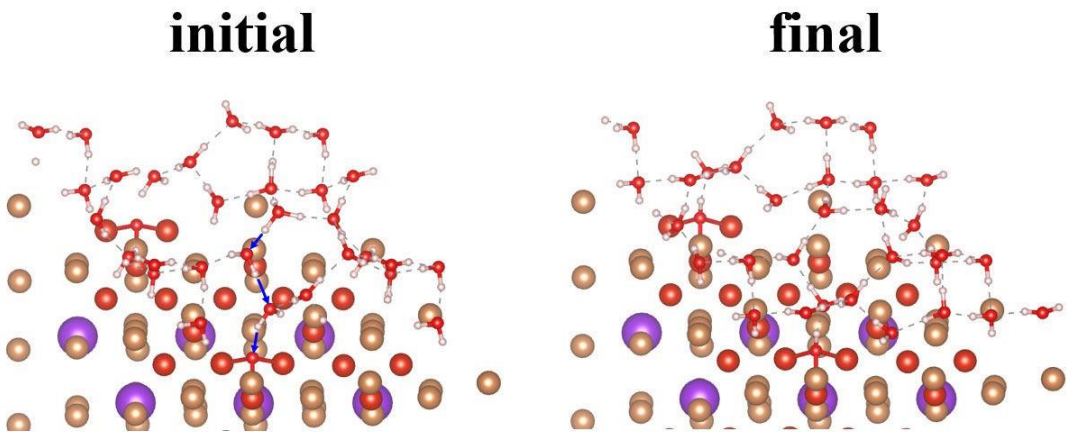

Fig. S7 The H-shuttle process of the O* → OH* step on the surface Sb2-VSb1 with an Sb vacancy.

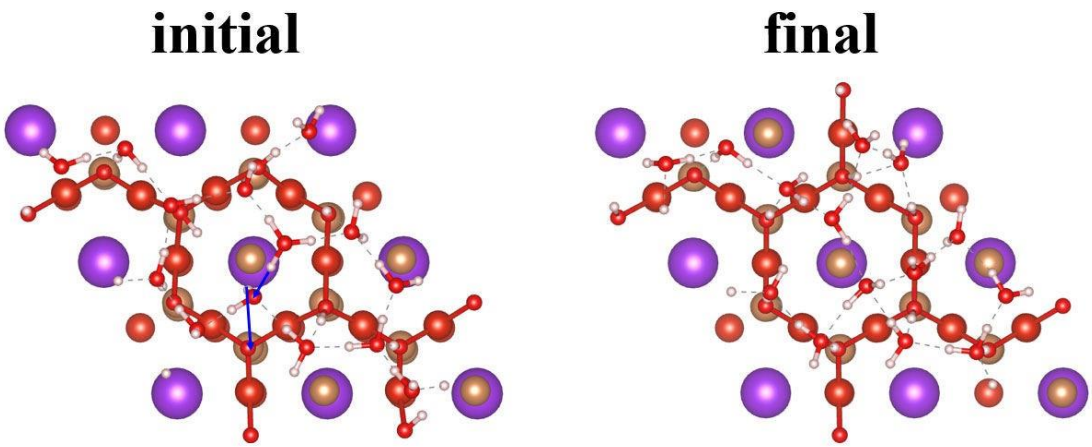

Fig. S8 The H-shuttle process of the O* → OH* step on the surface VSb1 with a 5:3 OH*:O* coverage.